High-spin spectroscopy in ^{125}Xe

A. Al-Khatib, G. B. Hagemann, G. Sletten, A. K. Singh, H. Amro, G. Benzoni, A. Bracco, P. Bringel, F. Camera, M. P. Carpenter, P. Chowdhury, R. M. Clark, C. Engelhardt, P. Fallon, B. Herskind, H. Hübel, R. V. F. Janssens, T. L. Khoo, T. Lauritsen, A. Neußer-Neffgen, and C. Rønn Hansen

Phys. Rev. C **83**, 024306 — Published 14 February 2011

DOI: 10.1103/PhysRevC.83.024306

High Spin Spectroscopy in ^{125}Xe.

A. Al-Khatib,[1] G.B. Hagemann,[2] G. Sletten,[2] A.K. Singh,[3] H. Amro,[4] G. Benzoni,[5] A. Bracco,[5] P. Bringel,[1] F. Camera,[5] M.P. Carpenter,[6] P. Chowdhury,[7] R.M. Clark,[8] C. Engelhardt,[1] P. Fallon,[8] B. Herskind,[2] H. Hübel,[1] R.V.F Janssens,[6] T.L. Khoo,[6] T. Lauritsen,[6] A. Neußer-Neffgen,[1] and C. Rønn Hansen[2]

[1]*Helmholtz–Institut für Strahlen- und Kernphysik, Universität Bonn, Nußallee 14-16, D-53115 Bonn, Germany.*
[2]*Niels Bohr Institute, Blegdamsvej 17, DK-2100 Copenhagen, Denmark.*
[3]*Department of Physics & Meteorology, Indian Inst.of Technology, Kharagpur, IN-721302, India.*
[4]*Univ. Michigan, Dept. Radiat. Oncol.,Ann Arbor, Mi 48109, USA.*
[5]*Dipartemento di Fisica and INFN, Sezione di Milano, I-20133 Milano, Italy.*
[6]*Physics Division, Argonne National Laboratory, Argonne, IL 60439, USA.*
[7]*Dept. of Physics, Univ. of Massachusetts, Lowell, Lowell Massachusettes 01854 USA.*
[8]*Lawrence Berkeley National Laboratory, Ca 94720 Berkeley, USA.*

Levels excited up to 39.8 MeV and 119/2 units of angular momentum have been populated in ^{125}Xe by the $^{82}Se(^{48}$Ca,5n$)^{125}$Xe reaction. High fold γ-ray coincidence events were measured, using the Gammasphere Ge-detector array. Nine regular rotational bands extending from levels identified previously, up to almost 60 $\hbar$, have been identified and 3 of these have been connected to low-lying levels having well established spins and parities. Configurations have been assigned to 6 of the bands based on alignment properties, band crossings and comparison with theoretical cranked shell model calculations (CSM). Transition quadrupole moments have been measured for these bands, in the spin range 31 - 55 $\hbar$ and found to be in agreement with the CSM calculations. The corresponding quadrupole deformation ϵ_2 ranges from 0.28 to 0.34 at a gamma deformation of 0° and from 0.29 to 0.36 at a gamma value of 5°.

PACS numbers: 21.10.-k, 21.10.Ky, 21.10.Hw, 23.20.Lv

I. INTRODUCTION

The level structure of ^{125}Xe at low spin and excitation has been studied in detail previously both experimentally and theoretically [1–5]. The most outstanding features of the structure is a γ softness at low and moderate spin and a large susceptibility to polarization effects from the excitation of quasiprotons and quasineutrons. For both protons and neutrons the unique parity $h_{11/2}$ intruder subshells play a dominant role. The alignment of $h_{11/2}$ protons drives the nucleus towards a prolate shape, while the alignment of $h_{11/2}$ neutrons induces an oblate deformation. The deformation driving properties of neutrons and protons are, therefore, conflicting and the nucleus may adopt either a prolate, oblate or triaxial shape, depending on the intrinsic configuration. A substantial amount of spectroscopic data has been provided at low and moderate spin for ^{125}Xe and neighboring nuclei concerning normal deformed (ND) nuslear shapes [1, 3, 5], but recent experiments at extreme spins, with the aim of identifying hyperdeformation, have given a wealth of new information. It has been shown that beyond roughly 20 units of angular momentum, the irregular structures typical for rapid changing shapes, become dominated by regular band structures extending another 20 to 30 units of spin [6]. This extension into the very high spin domain reflects the fact that the regular bands are the yrast structures and, therefore, receive the highest population in heavy ion fusion reactions. Since the present investigation is based on experimental results originating from the large data-set which was reported in [6], we refer to the introductory remarks in that paper for further considerations, and give in the next section only a short resume of the experimental procedure.

II. EXPERIMENTAL PROCEDURE

High spin states of Xe nuclei were produced by the reaction ^{82}Se(^{48}Ca,xn)$^{130-xn}$Xe at a beam energy of 205 MeV using the ATLAS accelerator at Argonne National Laboratory. Gamma-ray spectra were measured with the Gammasphere array equipped with 100 Compton-suppressed Germanium detectors [7] under the requirement of a coincidence fold of 5 or larger. Since the primary aim of the experiment was the measurement of discrete line spectra emitted from hyperdeformed nuclei produced with very small cross sections, the target should be able to withstand a very high beam intensity, and be thin enough to provide the best possible spectral resolution for fast transitions. The highly volatile Selenium target, therefore, presented a challenge and the details of the target technique is described in Ref. [6].

III. ANALYSIS AND RESULTS

A total of $2.8{\cdot}10^9$ events with a coincidence-fold condition of ≥ 5 was recorded and the Radware suite of programs [8] was used to create triple coincidence cubes and hypercubes (γ^4) for studies of coincidence relationships and the subsequent creation of the ^{125}Xe level scheme.

The relative spins of the states in the scheme were determined by an angular distribution analysis of cascading γ rays following the alignment in the reaction. In order to obtain the highest possible statistical accuracy, the ratio R_Θ was generated, as

$$< R_\Theta >= \frac{I_{forwd.-backwd.}}{I_{\sim 90^0}} \quad (1)$$

Two asymmetric coincidence matrices were built, one including all detectors on one axis and detectors close to average angles of 35° or 145° on the other. The second matrix was built with all detectors on one axis, but with the detectors near to 90° on the other. The ratio of peak intensities projected from these two matrices provides the angular intensity ratio R_Θ. For stretched quadrupole radiation $R_\Theta = 1.40\pm0.04$ is expected, while for stretched dipole transitions the ratio is 0.74 ± 0.02. Both numbers are obtained from averages of experimental R_Θ values for transitions of known multipolarity [2, 4]. For strong transitions in the lower part of the decay scheme, DCO ratios [9] were also used and these agree for selected cases well with the assignments by Granderath [4] and Seiffert [2]. For further confirmation, we refer to the discussion of bands 5 - 8 in chapter B where ratios around 0.6 and 1.0 for stretched dipole and stretched quadrupole transitions, respectively, are observed.

A. Lifetime measurements

The new long bands investigated in the present work extend quite high in spin and are found to have rather large transition energies. High-spin states in these bands are, therefore, associated with fast decays, i.e. the deexcitation occurs in flight during the passage of the recoiling ions through the target. In spite of the thin target fractional Doppler shifts of the gamma transitions could, therefore, be determined and used to extract state lifetimes in most of the long sequences. These lifetimes may be directly related to transition quadrupole moments which in turn can be compared to model predictions.

The fractional Doppler shift, F_τ, is related to the nominal gamma-ray energy, E^0_γ and the gamma-ray energy, $< E_\gamma(\theta) >$, observed at an angle θ, as

$$< E_\gamma(\theta) >= E^0_\gamma(1 + F_\tau \frac{v_{max}}{c})cos\theta \quad (2)$$

where v_{max} is the maximum recoil velocity, which can be calculated from the reaction kinematics. The relation of the observed $< E_\gamma(\theta) >$ to the angle (θ) allows for an estimate of F_τ. The extraction of lifetimes of the states in a band requires knowledge of the time dependence of the velocity, $v(t)$. This is obtained from known stopping power tabulations [10].

B. Level scheme

The level scheme of ^{125}Xe has been considerably extended from the versions obtained in earlier spectroscopic studies found in Refs. [1, 3, 5] and are proposed in Figs. 1 and 2. The most significant addition is comprised of a number of long bands with regular rotational structure - interrupted occasionally by crossings which, as in the case of ^{126}Xe, extend to rotational frequencies as high as $\hbar\omega \sim 1.2$ MeV and spins up to $\sim 119/2\hbar$ [6].

The labeling of the level structures in ^{125}Xe previously identified, vary from one author to the next and we have chosen to relate our labeling to the one of Granderath [1] in the following way : [1,2 = A,B], [3,4 = C,D], [5,6 = X,Y], [7,8 = Z], [9,10 = E,F], [11,11a,12 = G,H2,H1]. The long bands identified to very high spins are new in the present study and are labeled L1 to L6. Many of the known bands have been considerably extended in spin, and a few new medium-spin band structures have also been established. We have been able to confirm most of the previous spin and parity determinations [1] and to firmly determine spin and parity for bands 5,6 and 7,8, for which Refs. [1, 3] had different tentative suggestions. In the following, we give experimental arguments for spin and parity of the low-spin bands 5 - 8 and 13,14 and their extensions.

These new spin assignments provide agreement between the spin sequences in bands 5 - 8 and the suggested spins of Ref. [3] which were based on relative population intensities. A detailed knowledge of the low-spin band structures and their interconnections is crucial for establishing the decay routes from the newly identified long bands to the lower part of the level scheme. This allows, in most cases, for unique spin and parity assignment to these bands. In the present case, 3 of the long bands could be firmly connected.

The lowest spin positive parity bands 1 - 4 (labeled A,B and C,D in Ref. [1]) with firm spin and parity assignments, have not been modified or extended in the present work. They are, therefore, shown in Fig. 1, only with a few levels marked with labels 1, 3 and 4 to indicate how the medium-spin, positive-parity bands 5,6 and 7,8 decay. The decay routes which provide the spin and parity assignments to bands 5-8 are illustrated. Band 2 does not play any role in this issue and is not drawn in the figure.

The negative parity bands 9,10 also have firm spin and parity given in Ref. [1]. Bands 11,11a and 12 have been studied in Ref. [5], where spin and parity were determined from DCO ratios for $\Delta I = 1$ and 2 interband transitions to the yrast band 9. Bands 13,14 and their extensions are new, except for a single state in each of them which is observed to decay to states in a number of the low spin bands. [1, 5].

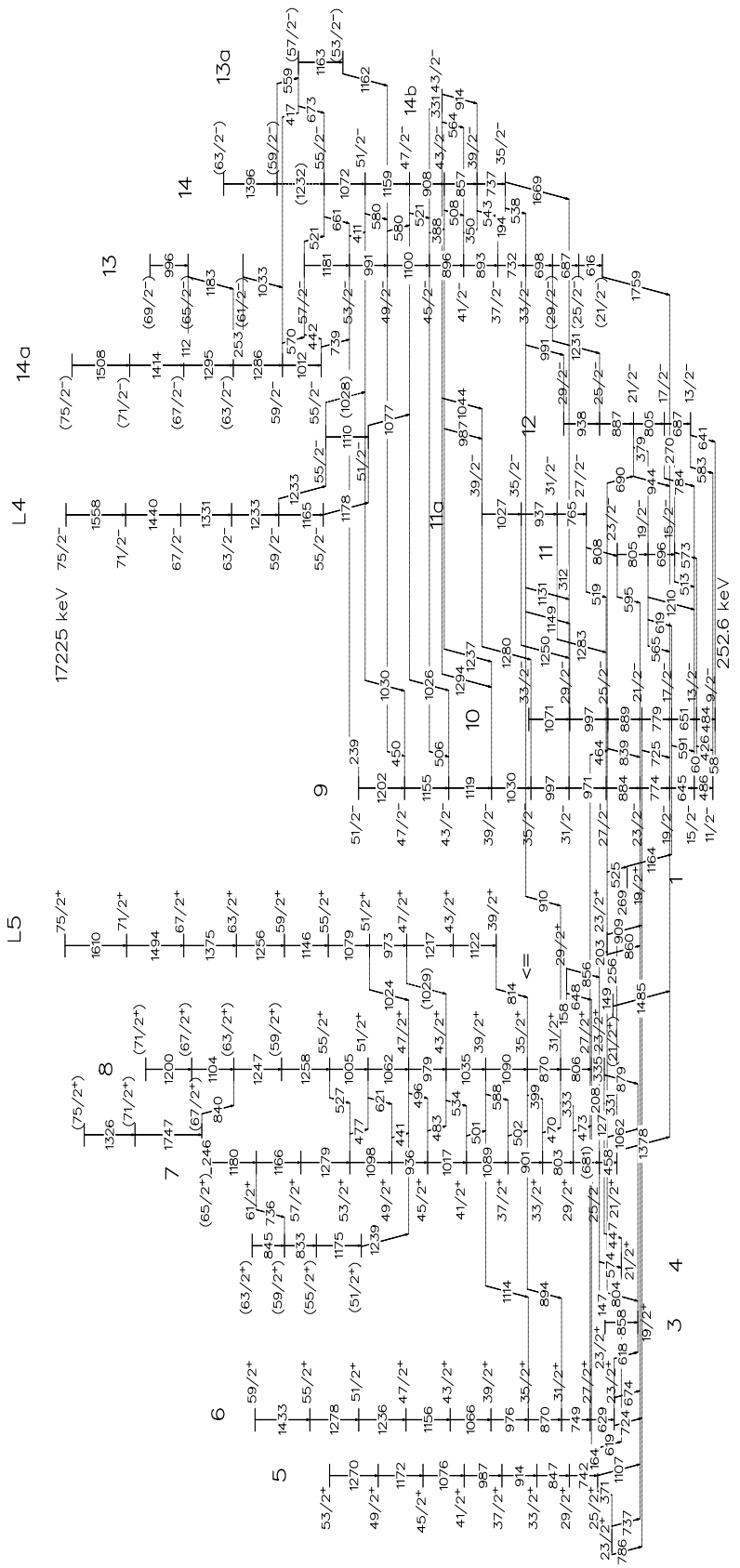

FIG. 1: Partial level scheme for ^{125}Xe at low and medium spin. Bands 1, 3 and 4 are only represented by the levels to which decay from bands 5,6,7 and 8 takes place. The arrow pointing to the $35/2^+$ level of band 8 refers to the very same level in Fig. 2 at a 5.162 MeV excitation energy.

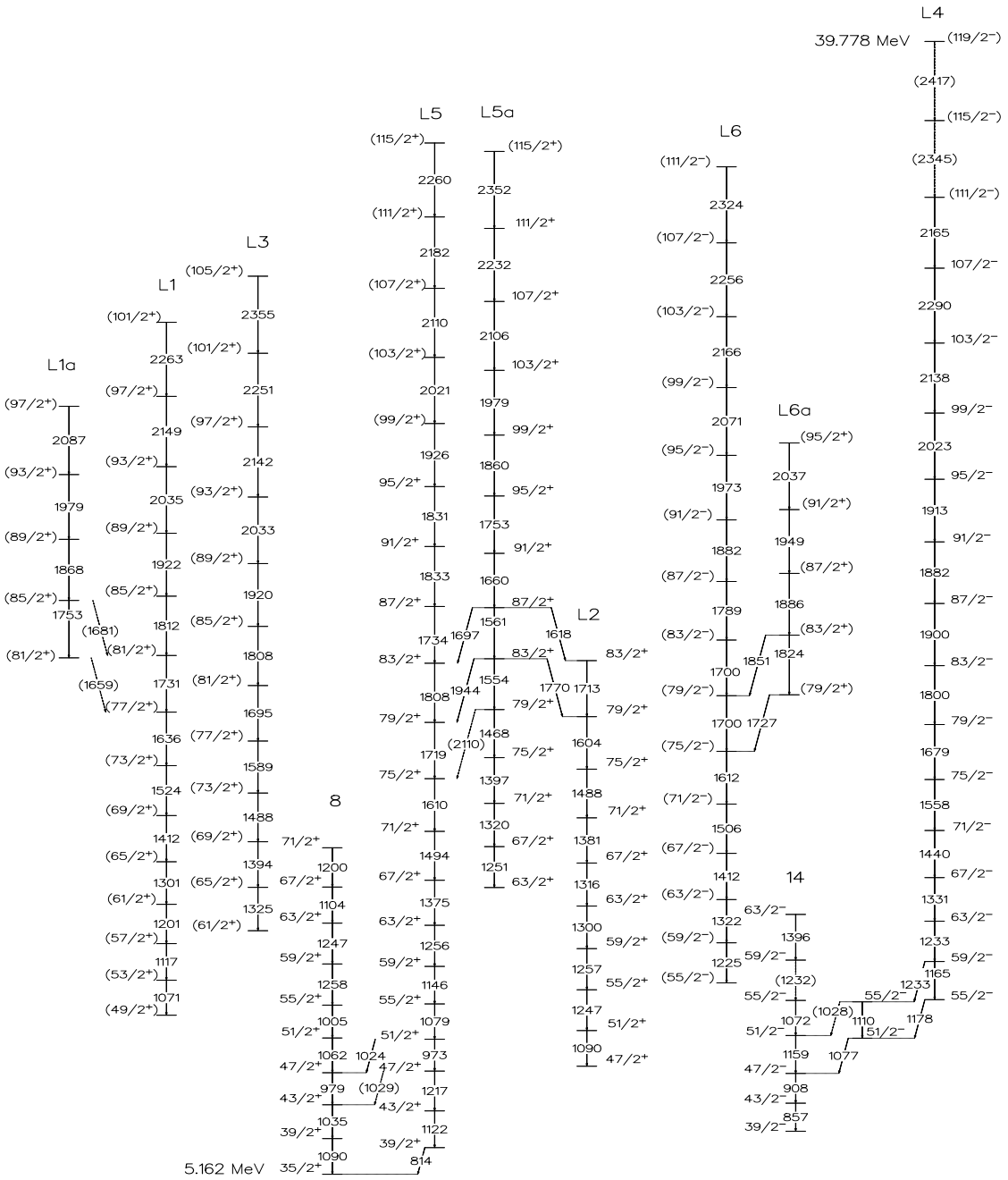

FIG. 2: Partial level scheme for the highest spins in ^{125}Xe. The excitation energy of the $35/2^+$ level of band 8 at 5.162 MeV is indicated as a link to the lower lying levels given in Fig. 1. The highest observed excitation energy is also marked. The spin and excitation energy of the unconnected bands, L1, L3 and L6 are estimates based on relative alignments, the spin of the highest, normal deformed lower levels to which they decay and the population strength.

1. *Band 7,8*

The lowest state in band 7, with spin $I^\pi = 21/2^+$ in Fig. 1, assigned as (19/2,21/2) in Ref. [1], decays by a 1378-keV transition to the $19/2^-$ level of band 9. The measured DCO ratio of 0.68(9) is consistent with a stretched dipole character. It is fed from the lowest state of band 8 by a 331-keV transition with a DCO ratio of 0.64(11). For the stronger of the other connections between bands 7 and 8 we list the following DCO ratios, all consistent with $\Delta I = 1$ transitions of (slightly) mixed M1/E2 character: For the 127-, 208-, 473/470- 399- and 502/501-keV transitions, the respective DCO ratios are: 0.68(8), 0.72(7), 0.52(4), 0.54(5) and 0.62(4). As a further support for the spin- parity assignment , the $21/2^+$ state of band 7 decays to the $19/2^+$ level of band 1 by a

269-keV transition with a DCO ratio of 0.63(18), and the $23/2^+$ level of band 8 decays by a 525-keV transition with a DCO ratio of 1.20(15) to the same $19/2^+$ level of band 1, consistent with a $\Delta I = 1$ and $\Delta I = 2$ character for those two transitions. By excluding the M2 transitions the positive parity of band 8 is thereby established. For Band 7, a 37/2 level at 5.664 MeV, which is very weakly populated, has been added to what was know previously, and both bands are extended to higher spin, including some irregular structures placed at the top.

2. Bands 5,6

The lowest state of band 5 with suggested spin $(21/2,23/2)\hbar$ in Ref. [1] decays by a 1107-keV transition with a DCO ratio of 0.56(23) to the $23/2^-$ level of band 9 and a 619-keV γ ray with a DCO ratio of 1.18(12) to the $21/2^+$ level in band 4, consistent with a $25/2^+$ assignment to this level. For the lowest state of band 6, assigned as (21/2) in Ref. [1], the most important decay transitions are at 724 keV with a DCO ratio of 0.77(9) to the $21/2^-$ state of band 10 and at 618 keV with a DCO ratio of 1.11(7) to the $19/2^+$ level of band 3, consistent with the $I^\pi = 23/2^+$ assignment to this level. Furthermore, bands 6 and 8 are observed to be connected by $\Delta I = 2$ transitions around $I = 35/2$, where the two bands come quite close in energy, interacting with each other, resulting in a measurable mixing which supports the fact that both pairs of bands have identical parity. Since band 8 has positive parity, positive parity is also proposed for bands 5 and 6. Both bands have been extended towards 30 $\hbar$.

3. Bands 13,14 and their extensions.

Bands 13 and 14 appear to correspond to a coupled structure with many $\Delta I = 1$ linking transitions. Band 14 exhibits $\Delta I = 2$ decay and band 13 $\Delta I = 1$ decay transitions to band 9 which indicates a mixing of bands 9 and 14, in particular around spin 47/2 $\hbar$. We take this observation as support for the spins and parity assigned to the bands. This assignment agrees with the identity of the $33/2^-$ state of band 13 and the $43/2^-$ level of band 14 with the quantum numbers proposed by Moon et al. [5], (band 4 and 5 in this reference). Several transitions from these two states connecting them to all the lower-lying negative parity bands are observed. At the highest spins, band 13 becomes very irregular, and band 14a which branches off band 14 becomes yrast after crossing with band 9 around spin $47/2\hbar$. This is illustrated in Fig. 11 and Fig .12.

4. The long bands.

The long bands extending to the highest transition energies and spins are presented in the partial level scheme of Fig. 2, together with selected parts of the lower spin bands to which decay has been established. The lowest excitation energy shown in Fig. 2, corresponding to the $35/2^+$ state of band 8, is indicated, which allows for a comparison to the low-medium spin structures of Fig. 1. The highest excitation energy, established in band L4 is also marked.

The long bands may be grouped according to their decay paths to either bands 7, 8 with positive parity or to bands 9 and 13,14 with negative parity. Bands L1, L3 shown in Fig. 3 belong to the first group. Bands L5, L5a and L2 are connected through an apparent interaction of close lying levels at $I = 83/2$. Band L5 could be connected to band 8 by 2 transitions of 1024 and 814 keV respectively. Spectra from sums of double coincidence gates in these three bands are presented in Fig. 4. The low energy part of Figs. 3 and 4 clearly indicate the similarity of the decay out properties of the first group of bands with the characteristic intense 203- and 208-keV transitions belonging to bands 7,8 at low spin.

Bands L4 and L6 belong to the other group, as demonstrated by the different low energy properties. These exhibit coincidence relations with intense transitions in band 9 in the spectra of sums of double gates placed on these bands (Fig. 5). Band L4 has been connected to band 14 at $I = 47/2$ and 51/2 by a stronger transition of 1077 keV and a weaker one of 1028 keV, respectively, through a 2-level structure with an $I = 55/2$ level close to the lowest ($I = 55/2$) state in band L4. The decay-out properties of bands L5 and L4 are illustrated by the spectra of Fig. 6. For the most intensely populated long bands, L3, L4, L5 and L5a, R_Θ ratios were established for most in-band transitions. For L4 and L5 R_Θ ratios were extracted also for the out-of-band transitions connecting them to the lower-spin bands. For band L3 stretched quadrupole character is confirmed for all in-band transitions up to and including the $(101/2) \rightarrow (97/2)$ 2251-keV transition. For band L4 stretched E2 character is confirmed for all in-band transitions up to and including the $107/2 \rightarrow 103/2$, 2290-keV transition, as well as for all transitions in and out of the 2-level structure between L4 and band 14, except for the weak 1028-keV transition. Band L5 has confirmed stretched E2 character for all in-band transitions up to and including the $95/2 \rightarrow 91/2$ 1831-keV transition as well as the 814-keV decay-out transition to band 8. For band L5a all in-band transitions up to and including the $111/2 \rightarrow 107/2$ 2232-keV transition as well as the two strongest γ rays connecting the band to band L5 are compatible with stretched E2 character.

These observations form the basis for the spin and parity assignments to states in bands L4 and L5 as proposed in Fig. 2. Band L5a has spins and parity determined

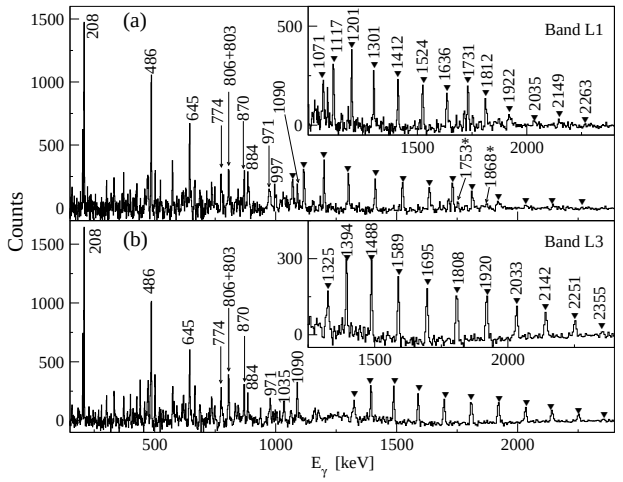

FIG. 3: Triple-gated, background-subtracted, γ-ray coincidence spectra showing transitions of bands L1 (a) and L3 (b) in ^{125}Xe. Each spectrum was generated by summing all possible combinations of triple gates of the form $(A \times A \times A)$ where A is a gate list of all transition energies of the related band. The filled triangles denote peaks of bands L1 and L3. Transitions from the side-branch L1a are marked with asterisks. The unmarked peaks with given energies belong to bands 8 and 9.

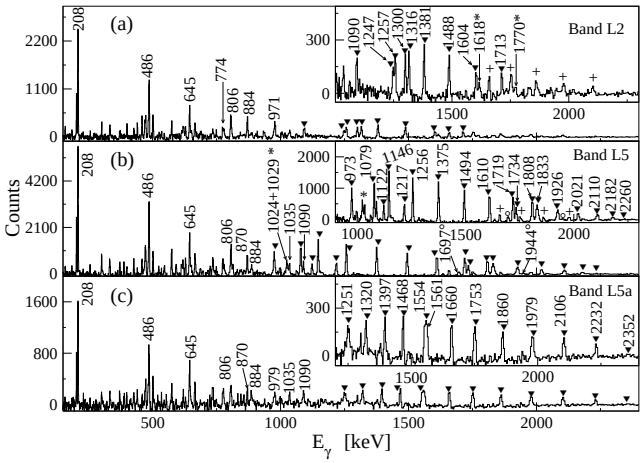

FIG. 4: Triple-gated, background-subtracted, γ-ray coincidence spectra showing transitions from bands L2 (a), L5 (b) and L5a (c) in ^{125}Xe. Each spectrum has been produced as described in the caption to Fig. 3. The unmarked transitions with given energies belong to bands 8 and 9. Filled triangles mark peaks of bands L2, L5 and L5a. The decay-out transitions are denoted with an asterisk. Transitions of band L5a are marked with a plus sign in (a) and (b). Open circles in (b) denote transitions from band L5a to band L5.

relative to band L5 through the E2 character of the connecting transitions. Band L2 is populated by decay from the $I = 87/2$ and $I = 83/2$ levels of band L5a. This decay structure indicates an interaction at the $I = 83/2$ level, which is a strong argument for a common spin and parity of this level and the one assigned to band L5a. For the transitions below the $I = 83/2$ level, stretched E2 character is assumed all the way, albeit R_Θ ratios are not available. Band L2 is already somewhat high in excitation energy relative to band L5 (see Fig. 11) and a change of the transition assignments to stretched dipole character would, however, increase the excitation energy further and is, therefore, considered unlikely.

Since the data include a large fraction of the 4n channel, leading to ^{126}Xe, together with the 5n channel under investigation here, there are many instances of contamination, and it has not been possible to obtain R_Θ ratios for the weaker populated long bands, L1, L2 and L6. The spin values for bands L1, L6 and L3 given in parentheses in Fig. 2 are suggestions based on alignments relative to those of the bands L4, L5 and L5a with firm spin determinations. Parities are suggested based on the similarity in the observed decay properties to either band L4 with negative parity or band L5 with positive parity.
The excitation energies indicated in Fig. 2 for the unconnected bands, L1, L3 and L6 are only tentative for the reasons discussed above, and were chosen according to the relative population as compared to the connected bands. These excitation energies may be questioned because of the resulting differences in spin and excitation energy with respect to the states in the ND bands to which they are observed to decay. Band L1 decays to bands 7,8 at $I = 39/2, 41/2$, which results in an energy difference of 3.3 MeV for a spin change of $4\hbar$ .For band L3 which populates bands 7,8 up to $I \sim 55/2$ the corresponding energy difference for $\Delta I = 4$ is chosen as 2.8 MeV. The same energy difference of 2.8 MeV for a spin change of $4\hbar$ is chosen for the placement of band L6, which decays to bands 9,14.

The relative population for the most intense gamma rays of the long bands have been estimated using the fitting procedure for gamma-ray intensity in the Radware analysis program. Intensities of the weaker gamma rays have been fitted in traditionally gated spectra and normalized to the Radware fits. The relative intensities are provided in Fig. 7. The intensity at $I \sim 35$ of band L4 represents $\sim 2\%$ of the lowest yrast transition, $15/2^- \rightarrow 11/2^-$ at 486 keV in band 9. In comparison, at the same spin, the strongest populated ND band, band 14a, has an intensity of $\sim 1\%$ of the 486-keV, $15/2^- \rightarrow 11/2^-$ transition.

C. Transition quadrupole moments of the long bands

Values of the fractional Doppler shift, F_τ, have been determined for several transitions in most of the long bands. As examples, F_τ values are shown vs. transition energy for bands L4, L5 and L5a in Figs. 8 - 10.

The Figs. 8 - 10 also show the results of the best fits from a simulation program, 'ft_fit_30' [11], in which the energy loss in the target of the projectile and the compound nucleus are simulated by means of the SRIM

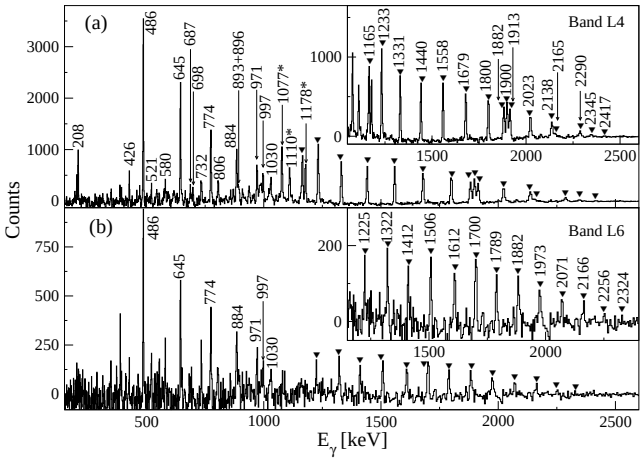

FIG. 5: Triple-gated, background-subtracted, γ-ray coincidence spectra for bands L4 (a) and L6 (b) in ^{125}Xe. Each spectrum has been generated as described in the caption to Fig. 3. The filled triangles denote peaks of bands L4 and L6 while the asterisks indicate possible decay-out transitions. The unmarked transitions with given energies belong to bands 8 and 9.

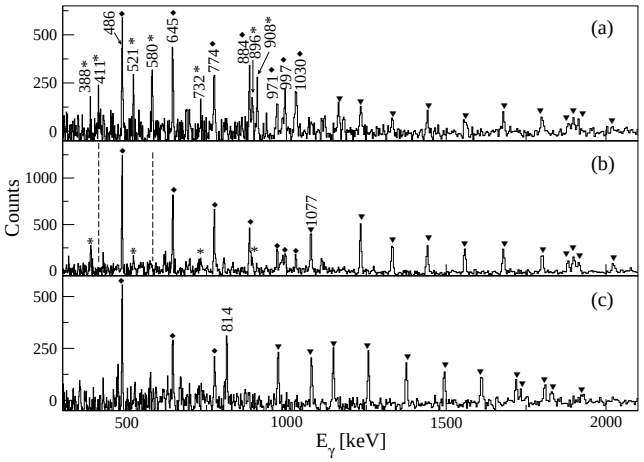

FIG. 6: Three panels showing triple gated spectra of bands L4 and L5 with the in-band transitions marked with filled triangles. Peaks marked with a filled diamond originate from band 9 and those marked with a star are transitions linking band L4 to low-lying transitions. The 814-keV transition in (c) links band L5 and L5a to the $35/2^+$ level of band 8. The gating condition in (a) requires 2 gamma-rays selected from all transitions in band L4 and a third one specified at 580 keV in band 13/14. The condition in (b) is 2 gamma-rays selected from all transitions in band L4 and a third one specified at 1110 keV in a structure just below band L4. The spectrum in (c) presents a logic "and" of two triple gated spectra with 2 gamma-rays selected from a list of all transitions, except for either the 1217 keV or the 1123 keV lines, in band L5, and the third one chosen at either 1217 keV or at 1123 keV, respectively. Both specified transitions are found at the bottom of band L5.

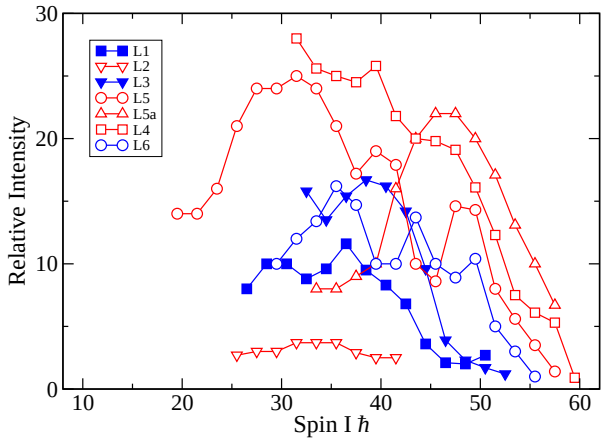

FIG. 7: (Color online) Relative intensities (arbitrary units) measured for the long bands.

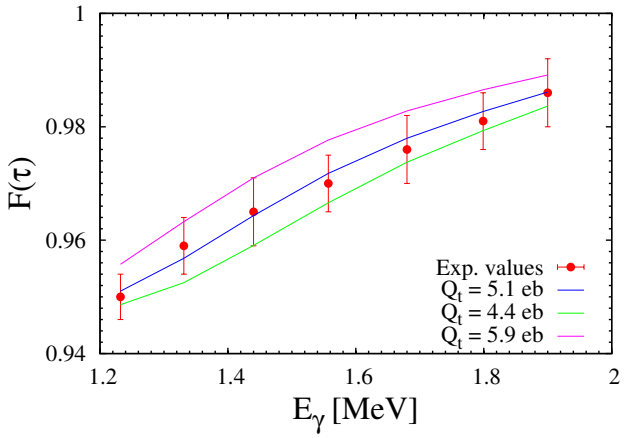

FIG. 8: (Color online) Fractional Doppler shift, F_τ, vs transition energy, E_γ, up to 1.9 MeV for band L4 with best fits shown for the transition quadrupole moment, Q_t.

program [12] using both electronic and nuclear stopping powers. The time profile in the γ decay of E2 transitions through the band depends, in addition to the transition energies, on two parameters: the transition quadrupole moment Q_t considered constant for the band, and a side-feeding transition quadrupole moment Q_{sf} which models unobserved side-feeding through bands assumed to be composed of transitions with similar transition energies as the band under analysis. The figures provide the best fits to the observed data, and Table I gives the extracted values of both Q_t and Q_{sf} for the strongest populated bands. In all cases the best fit is obtained with a value of Q_{sf} slightly lower than that of Q_t. Although the error bars are fairly large, the determined values are sufficiently precise to distinguish between different shapes corresponding to minima found in the Cranked

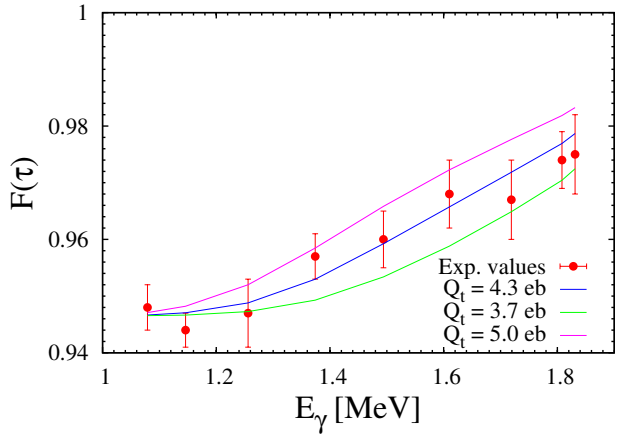

FIG. 9: (Color online) Fractional Doppler shift, F_τ, vs transition energy, E_γ, up to 1.9 MeV for band L5 with best fits for the transition quadrupole moment, Q_t.

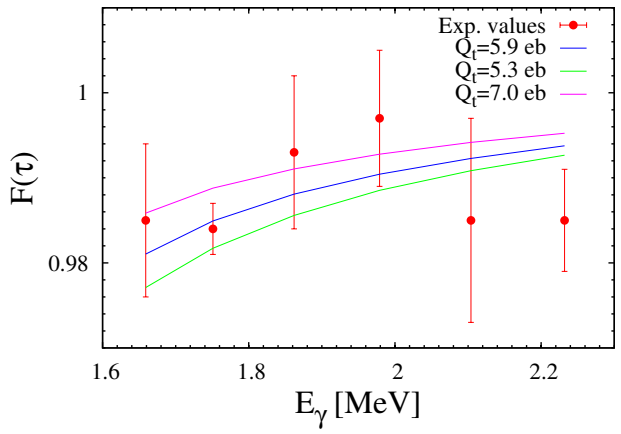

FIG. 10: (Color online) Fractional Doppler shift, F_τ vs transition energy, E_γ up to 2.2 MeV for band L5a with best fits shown for the transition quadrupole moment, Q_t.

Shell Model (CSM) calculation of potential energy surfaces.

IV. DISCUSSION

A. Structure of 'ND' bands

The shape of the nucleus at low spin depends strongly on the orbital occupied by the odd neutron. As pointed out in Ref. [1], the preferred shape related to an $h_{11/2}$ neutron is associated with a large negative value of $\gamma \sim -42°$, whereas the expected shape for the core with a neutron in one of the positive parity orbitals, $g_{7/2}$ or $s_{1/2}, d_{3/2}$ has a value of $\gamma \sim 2°$. In the two cases, moderate values of the quadrupole deformation parameter, $\epsilon_2 \sim 0.19$ and ~ 0.20, respectively, are expected.

Band	Spin range [$\hbar$]	Q_t [eb]	Q_{sf} [eb]	ϵ_2 $\gamma = 0°$	ϵ_2 $\gamma = 5°$
L1	32 - 40	$5.1^{+1.0}_{-1.0}$	$4.0^{+0.9}_{-0.7}$	0.29	0.31
L3	32 - 42	$5.4^{+1.1}_{-1.0}$	$4.2^{+1.0}_{-0.7}$	0.31	0.33
L4	31 - 43	$5.1^{+0.8}_{-0.7}$	$4.1^{+0.6}_{-0.7}$	0.29	0.31
L5	31 - 41	$4.3^{+0.7}_{-0.6}$	$3.4^{+0.6}_{-0.5}$	0.26	0.27
L5a	45 - 55	$5.9^{+1.1}_{-0.6}$	$4.7^{+0.9}_{-0.6}$	0.34	0.36
L6	31 - 45	$4.8^{+0.9}_{-1.0}$	$3.9^{+1.2}_{-0.9}$	0.28	0.29

TABLE I: Experimental transition and side-feeding quadrupole moments, Q_t and Q_{sf}, respectively, for the long bands. The corresponding quadrupole deformation, ϵ_2 is extracted for two values of the triaxiality parameter, γ. For bands **L1**, **L3** and **L6** parity and signature are tentative.

These shapes are only relevant below the first band crossings i.e., before excited quasiparticles are involved. The excitation of a pair of $h_{11/2}$ protons is expected to drive the core towards a prolate shape, with γ close to 0°, in contrast to the $h_{11/2}$ neutron excitations which drive the core towards negative gamma values.

For bands 9,10 based on the $\nu h_{11/2}$ orbital a second pair of $h_{11/2}$ neutrons may be expected to align whereas for the positive parity bands 1, 2 and 3, 4 alignment of the first pair of $h_{11/2}$ neutrons is unblocked and expected to occur. In competition with these two-quasineutron excitations, the first pair of $h_{11/2}$ protons may align as well.

The excitation energy of selected bands is shown relative to a rigid reference, $\mathrm{A}I\cdot(I+1)$, as a function of spin in Fig. 11. The relative alignment vs. rotational frequency $\hbar\omega$ are presented for the same bands, including the unconnected bands, L1, L3 and L6, in Fig. 12.

1. *Negative parity bands*

Bands 9, 10 comprise the favored and unfavored signature partners of the lowest $h_{11/2}$ neutron excitation. The alignment gain observed in band 9 at $\hbar\omega \sim 480$ keV has been interpreted as caused by the alignment of the second pair of $h_{11/2}$ neutrons [1]. Bands 11 and 12 at somewhat higher excitation energy have been interpreted [5] as being built on the second $h_{11/2}$ neutron excitation, presumably related to a shape with considerable softness in the gamma parameter.

In the spin range of $15-35\hbar$ the bands 13,14 with their extensions take over in terms of population. They attain an alignment gain of about 8 $\hbar$ relative to band 9 in the

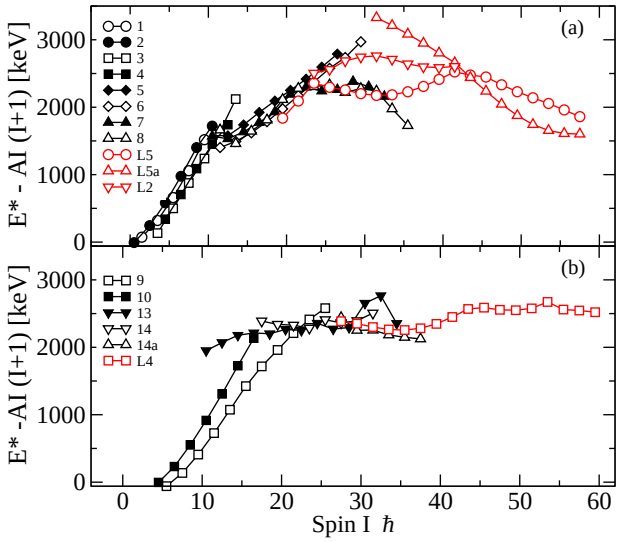

FIG. 11: (Color online) Excitation energy $E^* - AI(I+1)$ (keV) vs spin $I\hbar$, with A=10.35 keV. (a): Positive parity normal deformed bands 1, 2, 3, 4, 5, 6, 7, and 8, and connected long bands L5, L5a and L2. (b): Negative parity normal deformed bands 9, 10, 14, 13, 14a and the connected long band, L4. Closed and open symbols represent states with signature $\alpha = +1/2$ and $\alpha = -1/2$, respectively.

frequency range $\hbar\omega \sim 350 - 500$ keV frequency range, and we suggest that these bands correspond to the additional alignment of a pair of $h_{11/2}$ protons, which will most likely cause a change towards a prolate shape. Although band 14a appears to be rather regular, in the highest frequency range these bands are characterized by pronounced irregularities, which may illustrate the loss of a well-defined shape for collective excitations at the highest angular momenta. One should note though, that some of the irregularities are related to interactions between bands 9 and 14 at I-values below $\sim 43/2$ as well as between bands 14 and 14a at $I \sim 55/2$ - $59/2$, likely caused by accidental closeness in excitation energy.

In Ref. [5] the short band 11a was suggested to correspond to the $(h_{11/2})^2$ proton excitation built on band 9, but the present assignment of this excitation to bands 13,14 appears much more plausible due to the observation of the expected large alignment gain relative to band 9.

2. *Positive parity bands.*

Bands 1,2 with some signature splitting have been interpreted as being built on the $s_{1/2}, d_{3/2}$ neutron excitation, while bands 3,4 are proposed to be associated with the $g_{7/2}$ neutron excitation. For both one expects a close to prolate shape. Most likely, the onset of an alignment gain in these bands at a frequency $\hbar\omega \sim 370$ keV is caused by the alignment of the first pair of $h_{11/2}$ neutrons.

At higher spin, the population strength is concentrated in bands 5,6 and 7,8, which both decay at the bottom to the low-spin positive-parity bands, as well as to the yrast negative-parity band, band 9. The alignment gain relative to bands 1,2,3,4 is also close to 8 $\hbar$. We interpret this alignment gain of $8\hbar$ in bands 5 and 6 as the alignment of a pair of $h_{11/2}$ protons added to the basic $s_{1/2}, d_{3/2}$ structure. Likewise, bands 7 and 8, showing a more pronounced partnership with $\Delta I = 1$ connecting transitions, may be interpreted as built on the $g_{7/2}$ neutron excitation with an aligned pair of $h_{11/2}$ protons. Whether these higher spin bands also have the first pair of $h_{11/2}$ neutrons aligned, as indicated by the slight upbends in bands 1,2 and 3,4 at $\hbar\omega \sim 370$ keV remains an open question.

Bands 7,8 with the suggested configuration $\nu g_{7/2} \otimes \pi(h_{11/2})^2$ becomes irregular with a considerable alignment gain at $\hbar\omega \geq 500$ keV, whereas bands 5,6 with the configuration $\nu s_{1/2}, d_{3/2} \otimes \pi(h_{11/2})^2$ stay rather regular throughout the entire frequency range covered. Apparently, this latter configuration can accommodate more angular momentum before collectivity is lost.

B. Structure of long bands

The long bands may be related to the normal-deformed (ND) bands by consulting Figs. 11,12 which indicate first of all that the (connected) long bands compete with, and actually get quite close to the ND bands in the $25 - 35\hbar$ spin range. In contrast to the ND bands, which appear to be rather irregular in the region of overlap, the long bands show quite a smooth alignment behavior up to the highest observed frequencies, interrupted by alignment-gains presumably caused by crossings. It should be noted that the spin values given in Fig. 2 used for extracting the alignment presented in Fig. 12 are assumed values for the unconnected bands.

The dynamical moment of inertia, $\Im^{(2)}$, is presented for all the long bands in Fig. 13. The values seem to group around two values of $\sim 36\hbar^2\text{MeV}^{-1}$ for bands L1, L3, L4 and L5a, and $\sim 42\hbar^2\text{MeV}^{-1}$ for bands L5 and L6 for a frequency of 900 - 1100 keV. This grouping does not persist at lower frequency, where the general trend is a rise towards the lower end of the bands. Note that values of $\Im^{(2)}$ extracted at crossings as well as extreme values obtained at the very bottom of the bands have been omitted in the figure.

Transition quadrupole moments could be measured for all of the long bands, except for band L2 which only is observed below $I = 83/2$; see Table I. It is possible to compare these quadrupole moments to CSM calculations performed with the Ultimate Cranker code (UC) [13, 14]. The nuclear shape found from CSM calculations of local minima in Potential Energy Surfaces (PES) in practically all combinations of parity and signature in the even proton and odd neutron systems show a common feature. These minima correspond to values of the quadrupole deformation parameter, $\epsilon_2 \sim 0.35$ and values

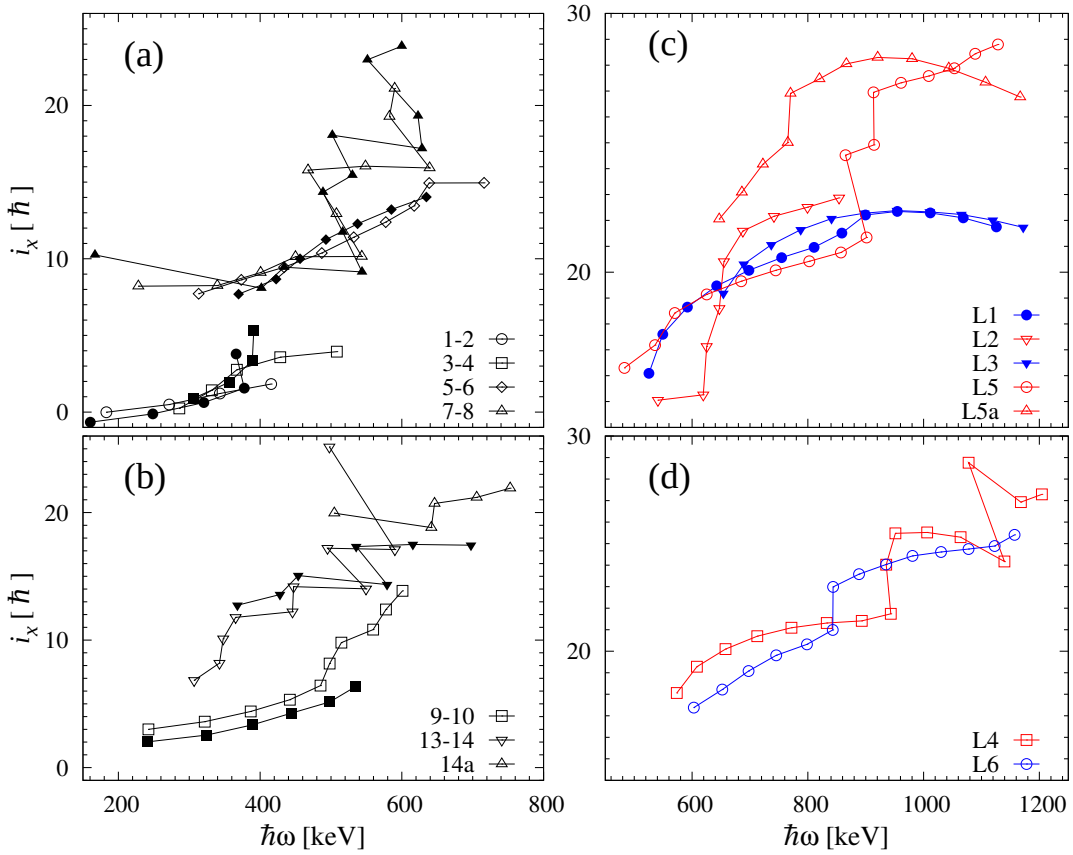

FIG. 12: (Color online) Aligned angular momentum, i_x, relative to a reference computed with Harris parameters, $(\Im_{(0)}, \Im_{(1)}) = (16\hbar^2 MeV^{-1}, 7\hbar^4 MeV^{-3})$, as a function of rotational frequency, $\hbar\omega$, for bands in ^{125}Xe. Panels for the normal deformed and long bands are shown in (a,b) and (c,d), respectively. Positive parity bands are shown in panels (a,c) while negative parity bands are shown in panels (b,d). Closed and open symbols represent bands with signature $\alpha = +1/2$ and $\alpha = -1/2$, respectively.

of the nonaxiality parameter $\gamma \sim 5^\circ$ in a large spin range of $\sim 25 - 60\hbar$, similar to the findings for ^{126}Xe, see Ref. [6] for details. An example is given in Fig. 14. The measured quadrupole moments for the long bands, converted to deformation parameters, ϵ_2, γ, are (within their fairly large errors) in excellent agreement with this predicted shape, as seen from Table I.

An analysis of the possible structure of the long bands in ^{125}Xe is naturally based on the orbitals available for neutron and proton excitations at $\epsilon_2 \sim 0.35$ and $\gamma \sim 5^\circ$. Their characteristic properties concerning alignments and crossings can be obtained from cranked shell model calculations of energies in the rotating system, e', as a function of rotational frequency for neutrons and protons (see Figs. 15 and 16, respectively). Only crossings at frequencies above ~ 0.6 MeV are considered relevant for the observed frequency range of the long bands. We note that the alignments visible from these figures may be overestimated, since the pairing used in the calculations, although decreased with frequency, may be overestimated for these rather large rotational frequencies.

In the neutron system, positive-parity excitations are based on the $i_{13/2}$ orbitals for which the first and second crossings are expected at $\hbar\omega \sim 0.58$ and 0.95 MeV, respectively. The latter crossing is expected to result in an alignment gain of $\sim 8.5\hbar$. Negative parity orbitals above $\hbar\omega \sim 0.6$ MeV are associated with the $h_{11/2}$ state, and at somewhat higher frequency of $\hbar\omega \sim 0.86$ MeV the negative signature of the $h_{9/2}$ orbital becomes favored, with a small associated gain of $\sim 1.2\hbar$..

In the proton system, above $\hbar\omega \sim 0.6$ MeV, the positive parity excitations may be based on the $g_{7/2}$ and $d_{5/2}$ orbitals which both show signature splitting, but with an opposite sign. At higher frequency, the routhian, e', of the $i_{13/2}$ orbital with a large negative slope becomes energetically favored. It may be expected to cross and interact with the positive signature branches of the $g_{7/2}$ and $d_{5/2}$ orbitals at frequencies of $\hbar\omega \sim 0.9$ MeV. The crossing causes in both cases an alignment gain of $\sim 5.3\hbar$. For the negative parity orbitals, the negative signature partner of the $h_{11/2}$ orbital is lowest with a large signature splitting and no crossings with large alignment gains are expected.

Crossings observed in the long bands are best visible in the plot of the relative alignment in Fig. 12. It should be noted, however, that some of the irregularities may be

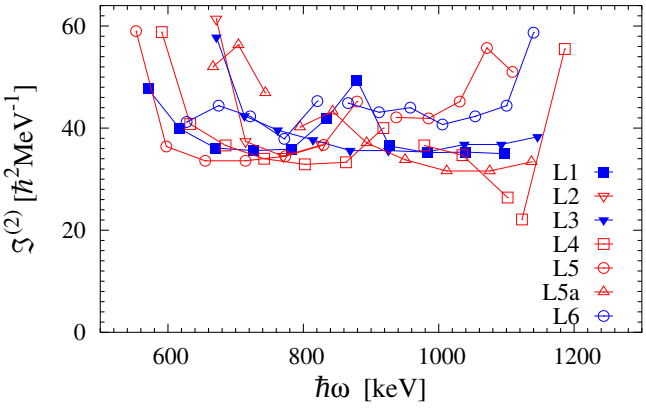

FIG. 13: (Color online) Dynamical moment of inertia $\Im^{(2)}$ vs rotational frequency, $\hbar\omega$, for all of the observed long bands. Extreme values at the bottom of some of the bands and at crossings have been omitted, resulting in discontinuities in some of the curves.

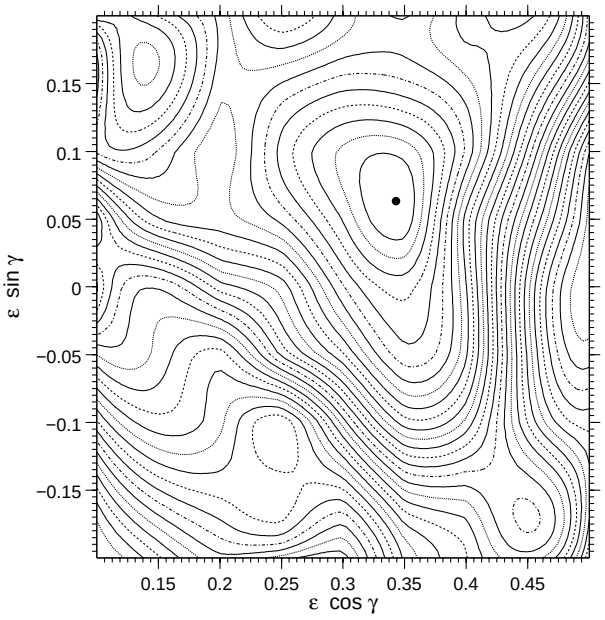

FIG. 14: Potential energy surface for the lowest configuration in ^{125}Xe with parity and signature $(\pi, \alpha) = (+, -1/2)$ (as in bands L5, L5a and L2) at spin $107/2\ \hbar$

due to accidental closeness in energy with states such as the 83/2 states in bands L5, L5a and L2.

The suggested single particle structure of the 7 long bands is discussed in details in the following subsections and summarized in Table II.

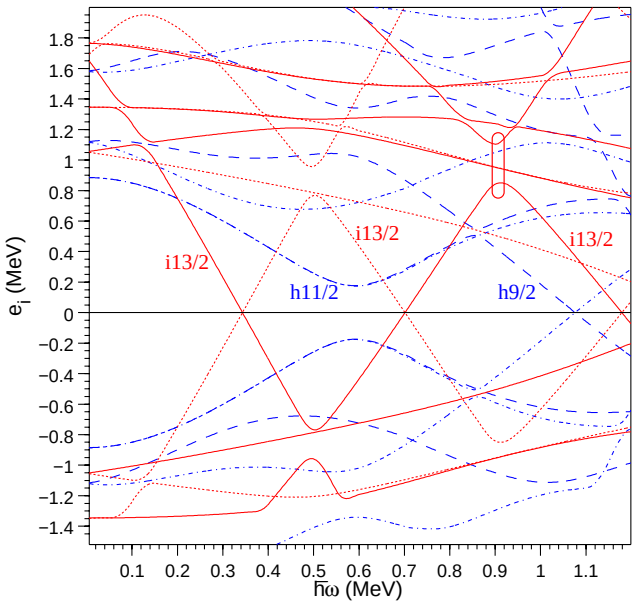

FIG. 15: (Color online) Excitation energy in the rotating frame, e', for neutrons as a function of rotational frequency, $\hbar\omega$, for ^{125}Xe at $(\epsilon_2, \gamma) \sim (0.35, 5^\circ)$. The e'-curves of parity and signature, (π, α) are given as solid lines for (+,+1/2), dotted lines for (+,-1/2), dashed lines for (-,+1/2) and dot-dashed lines for (-,-1/2). The box at $\hbar\omega \sim 0.9$ MeV marks the second $i_{13/2}$ crossing.

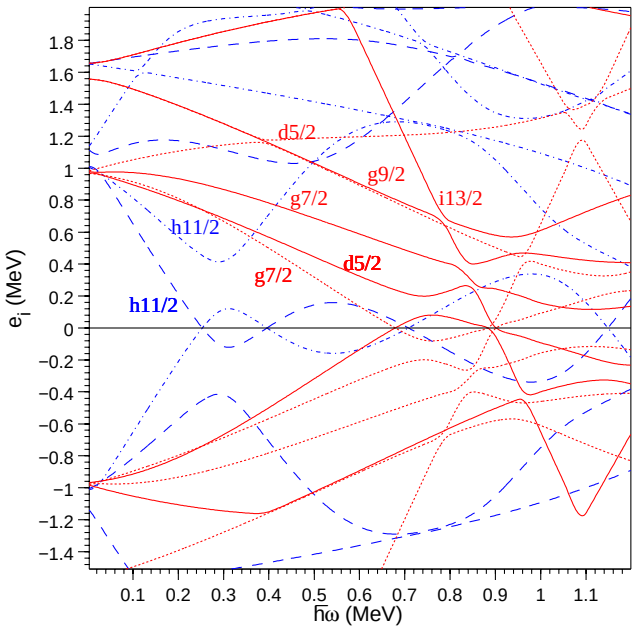

FIG. 16: (Color online) Excitation energy in the rotating frame, e', for protons as a function of rotational frequency $\hbar\omega$ for ^{125}Xe at $(\epsilon_2, \gamma) \sim (0.35, 5^\circ)$. The (π, α) convention is the same as in Fig. 15.

1. Band L4

Band L4 has quantum numbers $(\pi, \alpha) = (-, -1/2)$ and it experiences an alignment gain of $\sim 4\hbar$ at $\hbar\omega \sim 0.95$ MeV. Although slightly less than expected, we suggest that the alignment gain is caused by the excitation of an $i_{13/2}$ proton. The irregular behavior in i_x at $\hbar\omega \sim 1120$ keV introduces only a small gain in alignment and seems to be caused by a lift in energy of the $I = 107/2$ level. With no further large alignments occurring, the neutron system requires the second $i_{13/2}$ crossing to be blocked, which suggests the presence of an $h_{11/2}$ neutron coupled to a pair of $i_{13/2}$ neutrons.

Thus, the suggested configuration of band L4 can be written as

$\pi[g_{7/2} \times i_{13/2}]_{\alpha=0} \otimes \nu[h_{11/2} \times i^2_{13/2}]_{\alpha=-1/2}$

2. Bands L5 and L5a

Bands L5 and L5a have parity and signature $(\pi, \alpha) = (+, -1/2)$, and they exhibit some difference in both excitation energy and alignment behavior. Band L5a is yrast above spin $83/2\hbar$ where the two bands cross with each other and also with band L2, (see Fig. 11). Below this spin value, band L5a becomes increasingly non-yrast compared to band L5, approaching an energy difference between them of more than 1 MeV at the bottom of band L5a.

Band L5 experiences an alignment gain of $\sim 6\hbar$ at $\hbar\omega \sim 0.93$ MeV, whereas band L5a has gained a large alignment at a frequency of only 0.77 MeV. Below this frequency, the alignment gradually decreases. We suggest that the large alignment corresponds to the excitation of the second pair of $i_{13/2}$ neutrons, resulting in the neutron configuration $i^3_{13/2}$ with $(\pi, \alpha) = (+, +1/2)$. Most likely, the $i_{13/2}$ proton is also excited. To obtain total quantum numbers $(\pi, \alpha) = (+, -1/2)$ requires $(\pi, \alpha) = (+, 1)$ in the proton system, and, therefore, a second proton also with $(\pi, \alpha) = (+, +1/2)$ must be available. The most likely orbital is $d_{5/2}$.

Band L5a keeps the $i_{13/2}$ proton excitation below the frequency where the excitation occurs in band L5. The difference between L5 and L5a may be explained by the additional excitation of two extra neutrons, either a pair of $h_{11/2}$ neutrons (L5) or a mixed pair consisting of the same positive signature of $h_{11/2}$ and the negative signature of the $h_{9/2}$ neutron orbital (L5a). The energy difference between these two excitations is of the order of 0.5 MeV, which agrees with the energy difference between the L5 and L5a sequences at the highest spin values, see Fig. 11. This explanation agrees with the very similar alignments for the two bands at high spin and rotational frequencies.

For band L5 the proposed configuration at high spin is $\pi[i_{13/2} \times d_{5/2}]_{\alpha=1} \otimes \nu[h^2_{11/2} \times i^3_{13/2}]_{\alpha=+1/2}$,

and for band L5a at high spin the configuration is suggested to be

$\pi[i_{13/2} \times d_{5/2}]_{\alpha=1} \otimes \nu[h_{11/2} \times h_{9/2} \times i^3_{13/2}]_{\alpha=+1/2}$

At lower spin, the $i_{13/2}$ proton is replaced by the $g_{7/2}$ proton in band L5, whereas band L5a appears to keep the larger alignment of the $i_{13/2}$ proton further down in frequency.

3. Band L2

Band L2 with parity and signature $(\pi, \alpha) = (+, -1/2)$ could not be followed in spin beyond the crossing with bands L5 and L5a at $I = 83/2$. Presumably, it is weakly populated above this spin, where it most likely becomes higher in excitation energy than L5 and L5a. We, therefore, assume that no further increase of alignment takes place just above the maximum frequency at $\hbar\omega \sim 0.85$ MeV. At low frequency, in the region below $\hbar\omega \sim 0.85$ MeV, band L2 gains alignment resulting in a $\sim 2\hbar$ higher alignment than band L5. A plausible suggestion for the configuration of band L2 is therefore :

$\pi[h_{11/2} \times g_{7/2}]_{\alpha=-1} \otimes \nu[h_{11/2} \times i^2_{13/2}]_{\alpha=+1/2}$

The alignment gain at lower frequency must be caused by the first pair of $i_{13/2}$ neutrons, thus blocking the second pair of neutrons in this $i_{13/2}$ state. The excitation of the negative signature partner of the $g_{7/2}$ proton prevents the band from acquiring the $i_{13/2}$ proton alignment.

4. Bands L1 and L3

These two unconnected bands are proposed to have $(\pi, \alpha) = (+, +1/2)$. Band L3 is the most strongly populated of these two, and is presumably the lowest in excitation energy. Both bands appear to go through the frequency range up to 1.1 MeV without a gain in alignment comparable to the one observed for bands L4, L5 and L5a. The crossings responsible for those alignments must therefore be blocked in bands L1 and L3. This requires that the first pair of $i_{13/2}$ neutrons be excited, together with the favored negative signature partner of the $g_{7/2}$ proton state. The full configuration for band L3 is thus suggested to be

$\pi[h_{11/2} \times g_{7/2}]_{\alpha=-1} \otimes \nu[h_{11/2} \times i^2_{13/2}]_{\alpha=-1/2}$

For L1, we tentatively suggest an exchange of the signatures of the proton and neutron $h_{11/2}$ orbitals, with very little energy splitting in the neutron system, and a considerable energy difference (of the order of one MeV) in the proton system. The resulting configuration

$\pi[h_{11/2} \times g_{7/2}]_{\alpha=0} \otimes \nu[h_{11/2} \times i^2_{13/2}]_{\alpha=+1/2}$

is suggested for band L1.

Band	(π,α)	protons orbitals, signature	neutrons orbitals, signature
L4	(–,–1/2)	$i_{13/2}\cdot g_{7/2}$, 0	$h_{11/2}\cdot i^2_{13/2}$, –1/2
L5	(+,–1/2)	$i_{13/2}\cdot d_{5/2}$, 1	$h^2_{11/2}\cdot i^3_{13/2}$, +1/2
L5a	(+,–1/2)	$i_{13/2}\cdot d_{5/2}$, 1	$h_{11/2}\cdot i^3_{13/2}$ $\cdot h_{9/2}$, +1/2
L2	(+,–1/2)	$d_{5/2}\cdot g_{7/2}$, –1	$h^2_{11/2}\cdot i_{13/2}$, +1/2
L3	(+,+1/2)	$h_{11/2}\cdot g_{7/2}$, –1	$h_{11/2}\cdot i^2_{13/2}$, –1/2
L1	(+,+1/2)	$h_{11/2}\cdot g_{7/2}$, 0	$h_{11/2}\cdot i^2_{13/2}$, +1/2

TABLE II: Proton and neutron orbitals excited in bands L4, L5, L5a, L2, L1 and L3 at $\hbar\omega \sim 1$ MeV. Note that for bands L1 and L3 parity and signature are tentative.

5. Band L6

Band L6 is not connected, but tentatively assigned the same values, $(\pi,\alpha) = (-,-1/2)$, as band L4. It is presumably located at higher excitation energy. Band L6 does not experience the same alignment gain of $\sim 4\hbar$ at $\hbar\omega \sim 0.95$ MeV as band L4, but a smaller gain of about $1.5\hbar$ at $\hbar\omega \sim 0.85$ MeV. This indicates that $i_{13/2}$ crossings are blocked in both the proton, and the neutron systems. Since band L6 has no firm spin and parity assignment, we refrain from suggesting further details for its configuration, and band L6 is not included in Table II as a result.

C. Shape evolution with rotational frequency

The observed normal deformed bands cover a frequency range up to ~ 0.6 MeV with a maximum spin $\sim 35\hbar$. The lowest spin, one-quasineutron bands have the odd neutron occupying the lowest orbitals, e.g. $s_{1/2}, d_{3/2}$ for bands 1 and 2, $g_{7/2}$ for bands 3 and 4 and $h_{11/2}$ for bands 9 and 10. Compared to those bands the medium spin bands 5 and 6, 7 and 8 as well as 13 and 14 have much larger alignments corresponding to a 3- or 5-quasiparticle structure with a pair of $h_{11/2}$ quasiprotons and possibly also a pair of $h_{11/2}$ quasineutrons being excited. The shape of the core in these 3- or 5-quasiparticle bands is expected to be close to prolate with $\epsilon_2 \sim 0.2$. Bands 5 and 6 exhibit the most stable collective behavior, lasting up to $\hbar\omega \sim 0.62$ MeV, whereas the other bands have quite irregular patterns above $\hbar\omega \sim 0.5$ MeV, suggesting that the prolate shape with $\epsilon_2 \sim 0.2$ cannot sustain further quasiparticle excitations.

At still higher rotational frequency and spin, the nucleus is observed to undergo a change to an increased prolate deformation with a stability that allows 'long' bands to develop and be observed up to spins as high as $\sim 60\hbar$. The nuclear shapes expected from the UC calculations in this spin region are, indeed, in close agreement with the present measurements of transition quadrupole moments for the strongest populated 'long' bands, as seen from Table I. The table also indicates that the largest quadrupole moment of 5.9 eb exists at the highest spin, $I = 45-55$ in band L5a, which is yrast in this spin range, see Fig. 11. The larger prolate deformation above the crossing in band L5a may reflect the excitation of a deformation-driving $i_{13/2}$ proton and up to three $i_{13/2}$ neutrons. The corresponding feature could not be observed for band L5, for which the smaller quadrupole moment, 4.7 eb, is extracted below the $i_{13/2}$ neutron and proton crossings.

The sizable prolate nuclear deformation related to the long bands is also reflected in the dynamical moments of inertia displayed in Fig. 13. On average, the observed values of $\Im^{(2)}$ are $\sim 40\hbar^2\mathrm{MeV}^{-1}$. The expected value for rigid rotation of an ellipsoid with an axis ratio of ~ 1.3, corresponding to the extracted values of ϵ_2, is $\sim 56\hbar^2\mathrm{MeV}^{-1}$ [6]. We also note that the value of the parameter 'A' used in Fig. 11 corresponds to $\Im^{(2)} = 48.5$ $\hbar^2\mathrm{MeV}^{-1}$. In comparison, the value obtained from the global liquid drop calculation introduced in Ref. [15] vary between 42 and 48 $\hbar^2\mathrm{MeV}^{-1}$ for spins between 25 and 55 $\hbar$. Although the average experimental values are somewhat lower, it seems that two of the bands, L5 and L6, approach the 'global' calculated value [15] at the highest spins.

In the spin range of 40-50 $\hbar$ the excitation energies found for the connected long bands are in qualitative agreement (within a couple of MeV) with expectations from the UC calculations. It remains a puzzle, however, that the lowest lying structure predicted by the UC calculations in the spin regime of the long bands, is not identified experimentally. This band is expected to have $(\pi,\alpha) = (+,+1/2)$ with the odd neutron in the $i_{13/2}$ orbital and an additional pair of $i_{13/2}$ neutrons excited, as suggested for bands L5 and L5a. For the proton configuration, the orbitals are e.g. $i_{13/2}$, $g_{7/2}$ parents as suggested also for the L4 band. We refer to Fig. 11 and Table II. In the table, we observe that band L3 would be a possible candidate for the lowest lying band in so far as the $(\pi,\alpha) = (+,+1/2)$ assignment is concerned. This band is not connected to the low lying structures which makes its placement in the spin-energy space uncertain, see caption to Fig. 2. From Fig. 7, however, we conclude that an yrast position of band L3 would be in conflict with the measured intensity.

To investigate a possible misassignment of spin and excitation energy to the floating band L3, we have attempted an addition of 6 $\hbar$ to the spin of band L3 given in Fig. 2, in order to make its alignment similar to the values observed for bands L5 and L5a at high spin. The alternative version of Fig. 7 corresponds then to a shift

to higher spin by 6 $\hbar$ of the intensity distribution for band L3. However, the band is still too weakly populated for a structure which from the UC calculations would be expected to be clearly yrast. In addition, band L3 does not show the onset of the large alignment at $\hbar\omega \sim 0.9$ MeV related to the excited $i_{13/2}$ proton and neutrons of this expected yrast configuration. The puzzle therefore remains, and an expected, lowest lying, $(\pi, \alpha) = (+, +1/2)$ band with excited $i_{13/2}$ proton and neutrons has not been identified experimentally.

V. SUMMARY

The level structure of ^{125}Xe has been investigated to higher spin and higher excitation energy than was previously the case. A shape evolution with increasing rotational frequency is clearly demonstrated. This manifests itself by the appearance of regular rotational bands with transition quadrupole moments Q_t measured to be as large as 4.3 - 5.9 eb. In the 20-30 $\hbar$ spin region, they coexist with bands at "normal" deformation and extend to very high spins and frequencies. A total of 9 bands are identified. The rapid rotation results in alignment of quasi- neutrons and protons and the frequency at which the alignments take place has provided clues to specific quasiparticle assignments. On the basis of comparisons with theoretical calculations (UC), assignments of the high angular momentum orbitals in both the neutron and proton structures have been suggested for most of these bands. The long bands have quadrupole moments consistent with calculated deformations. The yrast band at high frequency, L5a, has the largest Q_t moment measured above the predicted and observed $i_{13/2}$ proton as well as $i_{13/2}$ neutron crossings. An inconsistency between the analysis of the experimental results and the theoretical calculations is observed concerning the predictions of the structure of the yrast band at high spin.

VI. ACKNOWLEDGMENTS

The authors thank the ANL operations staff at Gammasphere and in particular J.P. Greene for help in the target preparation. This work has been supported by the Danish FNU council for the natural sciences, by the German BMBF under contract no. 06 BN 109, the Alexander von Humboldt foundation, Germany and the U.S. Department of Energy, Office of Nuclear Physics, under contracts DE-AC02-06CH11357 (ANL) and DE-AC03-76SF00098 (LBNL).

VII. REFERENCES

[1] A. Granderath, D. Lieberz, A. Gelberg, S. Freund, W. Lieberz, R. Wirowski and P. von Brentano, Nucl. Phys. **A524**, 153-178 (1991).

[2] F. Seiffert, W. Lieberz, A. Dewald, S. Freund, A. Gelberg, A. Granderath, D. Lieberz, R. Wirowski and P. von Brentano, Nucl. Phys. **A554**, 287, (1993).

[3] I. Wiedenhöver, J. Yan, U. Neuneyer, R. Wirowski, P. von Brentano, A. Gelberg, N. Yoshida, and T. Otsuka, Nucl. Phys. **A582**, 77 - 108, (1995).

[4] A. Granderath, P.F. Mantica, R. Bengtsson,R. Wyss, P. von Brentano, A. Gelberg and F. Seiffert, Nucl. Phys. **A597**, 427 (1996).

[5] C.-B. Moon, C.S. Lee, T. Komatsubara, Y. Sasaki and K. Furuno, Phys. Rev.C **76**, 067301, (2007).

[6] C. Rønn Hansen, G. Sletten, G.B. Hagemann, B. Herskind, D.R. Jensen, P. Bringel, C. Engelhardt, H. Hübel, A. Neußer-Neffgen, A.K. Singh, M.P. Carpenter, R.V.F. Janssens, T.L. Khoo, T. Lauritsen, P. Bednarczyk, T. Byrski, D. Curien, G. Benzoni, A. Bracco, F. Camera, S. Leoni, R.M. Clark, P. Fallon, A. Korichi, J. Roccaz, A. Maj, J.N. Wilson, J.C. Lisle, T. Steinhardt, O. Thelen and S.W. Ødegård, Phys. Rev.C **76**, 034311, (2007).

[7] R.V.F. Janssens and F.S. Stephens, Nucl. Phys. News **6**, 9 (1996).

[8] D.C. Radford, Nucl. Instrum. Methods Phys. Res. **361A**, 297 (1995).

[9] K.S. Krane, R.M. Steffen and R.M. Wheeler, Nuclear Data Tables **11** (1973) 351.

[10] J.F. Ziegler, J.P. Biersack and U. Littmark, The stopping and Ranges of Ions in Matter, vol.1 (Pergamon, London 1985).

[11] F.E. Moore: Proceedings of the Workshop on Gammasphere Physics (World Scientific Publishing Co., Singapore, 1996)

[12] SRIM, The Stopping and Range of Ions in Matter, URL http://www.srim.org/

[13] T. Bengtsson, Nucl. Phys. **512**, 124 (1990); **A496**, 56 (1989).

[14] R. Bengtsson, http://www.matfys.lth.se/ ragnar/ultimate.html.

[15] B.G. Carlsson and I. Ragnarsson, Phys. Rev. C74, 011302(R) (2006) and I. Ragnarsson, Private communication